Low-Frequency Vibrations and Their Role in Ultrafast Photoisomerization Reaction Dynamics of Photoactive Yellow Protein

Haik Chosrowjan,[†,||] Seiji Taniguchi,[†] Noboru Mataga,[*,†] Masashi Unno,[‡,||] Seigo Yamauchi,[‡] Norio Hamada,[§] Masato Kumauchi,[§] and Fumio Tokunaga[§]

Institute for Laser Technology, Utsubo-Hommachi 1-8-4, Nishiku, Osaka 550-0004, Japan, Institute for Multidisciplinary Research for Advanced Materials, Tohoku University, Sendai 980-8577, Japan, and Department of Earth and Space Science, Osaka University, Toyonaka, Osaka 550-0043, Japan

Received: September 30, 2003; In Final Form: December 15, 2003

Low-frequency vibrational modes of the native photoactive yellow protein (PYP) and its several mutant and analogue systems have been investigated in "time" (femtosecond fluorescence up-conversion) and "frequency" (resonance Raman spectroscopy) domains to elucidate their role in ultrafast photoisomerization reaction dynamics of PYP. The oscillatory frequencies derived from time-domain analysis are in fair agreement with those obtained independently using spontaneous resonance Raman spectroscopy. Tentative assignments of the oscillatory components to particular vibrations are proposed supported by normal-mode calculations based on density-functional theory and ab initio MO methods. It is concluded that the out-of-plane skeleton bending mode of the chromophore, γ_{16}, is responsible for the observed oscillations in native and all mutant PYPs ($f_1 \approx 135$ cm^{-1}), while in-plane ν'_{42} and ν'_{43} modes are probably responsible for oscillations observed in the PYP analogue with locked chromophore. The low-frequency mode ($f_2 \approx 50$ cm^{-1}) present in time-domain experiments of all systems examined could not be fully characterized. A dynamic model called "trigger mode mediated guidance" has been proposed to explain in simple terms the ultrafast primary process initiating PYP's photocycle. This work provides a framework for future investigations on PYP's low-frequency vibrational modes in connection with its primary structural photodynamics.

Introduction

Photoactive yellow protein (PYP), discovered in 1985,[1] is a small (125 amino acids, 14 kDa), water-soluble protein with excellent physico- and photochemical stability. Its chromophore, 4-hydroxycinnamic acid (4HCA, referred also as *p*-coumaric acid), is covalently bound to the protein backbone at the sole Cys69 position via a thiolester linkage.[2,3] Because of several well-established heterologous overproduction procedures for holo-PYP in *Escherichia coli* and in vitro reconstitution of apo-PYP,[4−6] this protein has now become a model system for studies[7−22] in photochemistry and protein folding to the extent comparable with the rhodopsins.[23−28]

Photoexcitation of PYP with a blue light triggers a photocycle that involves several intermediate states.[7−10] For many photoreceptors, including also PYP, photoisomerization of the chromophore buried in the protein has been identified as the primary photoreaction triggering its photocycle. The initial isomerization event usually occurs on the several hundred femtoseconds time scale.[11−22,25−28] Detailed understanding of this primary response of a photoreceptor to light absorption is a prerequisite for understanding the formation of its signaling state at a later time on the molecular level. Among these proteins, PYP is the most stable, has the simplest structure, and shows a relatively simple photoreaction cycle, making it an ideal candidate for detailed elucidation of the dynamics and mechanisms of the ultrafast primary processes. Different time-resolved measurement techniques have been applied to understand and explain the mechanisms of the initial photoisomerization reaction in native PYP,[11,12,21,22] its mutants and analogues,[13−15,20] and several chromophore models in the water environment.[14,29,30] Furthermore, by diverse experimental studies[8,9,14,15,31−33] and quantum mechanical calculations,[34,35] it was demonstrated that PYP's photocycle is initiated by flipping the carbonyl group of the chromophore rather than its bulky aromatic ring. This result implies that the chromophore isomerization requires only minor rearrangements of the chromophore/protein structures in protein nanospace[14,15] (PNS, defined as the area including the chromophore and the nearby group of amino acids surrounding it) during the initial ultrafast events in the photocycle. Here we refrain from detailed comparisons of results presented in above cited works and refer the reader to the recent review articles[36] where up to date research on PYP and related systems is presented.

It should be noted here that the time-resolved fluorescence spectroscopy proved itself to be a powerful tool for investigations on the primary steps in the photoreactions of photosensitive proteins. It is especially effective for studies on systems undergoing ultrafast structural deformations (trans to cis or vice versa). In such systems, the fluorescence decay rate directly mirrors the photoisomerization rate because the product states (twisted state) in most cases are very weakly fluorescent or nonfluorescent.[37] It is also straightforward in comparison with transient absorption spectroscopy, which for complex systems such as PYP yielded different, in part even contradicting results.[9,16,17,36]

In relation to the important role of the PNS for the ultrafast reaction of the chromophore, it should be noted here that our

* Author to whom correspondence should be addressed. E-mail: haik@ile.osaka-u.ac.jp. Fax: ++81-664925641.
† Institute for Laser Technology.
‡ Tohoku University.
§ Osaka University.
|| Both authors contributed equally to this work.

10.1021/jp031126w CCC: $27.50
Published on Web 01/31/2004

femtosecond fluorescence decay dynamics studies on PYP indicated an ultrafast twisting reaction in a vibrationally nonrelaxed state. Namely, the system is elevated by a blue light absorption into the FC (Franck−Condon) excited electronic state with excess vibrational energy due to a number of intrachromophore vibrational modes. FC → Fl (Fluorescence state) conversion takes place rapidly accompanied with ultrafast IVR (intramolecular vibrational redistribution) leading to the Fl state with selectively excited coherent vibrational modes. Previously, indirect evidence concerning the involvement of coherent vibrational modes in photoisomerization reactions of bacteriorhodopsin,[25] bovine rhodopsin,[28] as well as PYP[11,15] has been gained from time-resolved fluorescence studies. For instance, the fluorescence dynamics in all three mentioned proteins are nonexponential; no dynamic Stokes shift but a slight narrowing of the fluorescence spectra within the first few picoseconds of the reaction were observed. It was then predicted that this narrowing effect most probably originated due to damping of coherently coupled intrachromophore modes and/or low-frequency vibrations of environmental protein interacting with chromophore along the twisting coordinate.[14,15] With increased time resolution of the measurements, the predicted oscillatory behavior in fluorescence dynamics was recently verified by two different experimental sets, first by the fluorescence up-conversion technique in native PYP and its seven mutants[18,19] and later by an optical Kerr-gate spectroscopy in native PYP.[22] Since these oscillations disappear in the denatured (unfolded) PYP owing to the ultrafast damping in the completely disordered environment, the well-ordered environment in PNS seems to be a prerequisite for its action in the ultrafast primary photoinduced reaction. In this respect, we are now developing detailed studies for the elucidation of the nature of low-frequency vibrations of PYP coupled with the fluorescence decay in the photoinduced twisting process of the chromophore in PNS. Namely, what role do the *low-frequency* intraprotein vibrations play in these early events?[38] Following simple considerations emphasizes their potential importance. A flipping, twisting, or complete isomerization of the chromophore in a given photoresponsive protein is a presumably *unidirectional* structural deformation occurring on a characteristic time scale. Hence, specific low-frequency intrachromophore vibrational modes (constituting *periodic* structural deformations) with periods on the same or comparable time scale could be effectively coupled to isomerization and play a crucial role in starting and "guiding" or "disturbing" the later reaction. For instance, in the case of PYP, the fastest twisting (or flipping) reaction occurs on an ∼300-fs (∼50%) time scale; thus, vibrational modes (if any) with periods in the 100-fs−1-ps time region (corresponding frequencies between 33−330 cm^{-1}) could be of special importance. To our best knowledge, there are no studies on PYP or related systems to identify and assign the low-frequency intraprotein vibrations in the 30−330 cm^{-1} spectral region.

Although the observed oscillations in the fluorescence decay dynamics of PYP are an interesting physical phenomenon, it still remains to be demonstrated that they are important for understanding the early events in PYP photoreaction. The first step in this direction would be the firm assignment of observed oscillatory modes, however, "time"-domain experiments alone seem not to be sufficient for unambiguous assignment of the coherence to particular vibrational mode(s). Vibrational spectroscopy, on the other hand, such as IR absorption and Raman scattering methods, is more suitable for this purpose. In our special case, where the emphasis is put on observation of *low-frequency* vibrations, resonance Raman (RR) spectroscopy seems to be advantageous over IR methods because measurements in the low-frequency spectral region with later technique, especially on biomolecules, bear a major difficulty arising from the strong absorption of water. One should note, however, that the comparison between observations from transient fluorescence and RR scattering techniques are not straightforward. It is simply because oscillations observed in time-resolved fluorescence decays originate from the excited electronic state, while the later technique probes the vibrational modes in the ground state of the given system. Nevertheless, supported by density-functional theory (DFT) and ab initio MO calculations, such a comparison is a justified approach to disclose origins and roles of low-frequency modes coupled with the primary photoisomerization reaction of the PYP (the important precautions for such comparison have been detailed in the DFT and ab initio MO calculations; correlations between time- and "frequency"-domain observations subsection).

Previous studies have reported the higher-frequency (above 600 cm^{-1}) region of the RR or FT Raman spectra of PYP_{dark} and its several photocycle intermediates.[34,39−43] Among other findings, it was shown that the frequency of the C8−C9 stretching mode ν_{29} depends on trans ($\nu_{29} \approx 1053$ cm^{-1}) to cis ($\nu_{29} \approx 990$ cm^{-1}) isomerization around the C7═C8 bond,[34,39] designating it as a structural marker or a "fingerprint" mode for trans/cis isomerization *state* of the chromophore. One aim of this work was to find (if any) the *dynamic* "fingerprint mode(s)" of the intrachromophore and/or chromophore−apoprotein coupled vibrations sensitively affecting the photoisomerization process and could be designated as "trigger" mode(s) for trans/cis isomerization. Existence of such "trigger" modes would explain in simple terms how the energy that is initially localized in a "hot" chromophore is channeled to trigger start the flipping, catalyzing a single reaction pathway so efficiently and avoiding the unwanted side reactions.

In this work, we determined experimentally low-frequency vibrational modes of the native PYP, its mutants, isotopomers, as well as denatured PYP for the first time and propose a tentative assignment of observed modes. Additionally, we have found correlations between data obtained from both time- and frequency-domain experiments and discuss the role(s) of low-frequency intraprotein vibrations in ultrafast photoisomerization reaction dynamics of PYP and related systems.

The composition of this paper is as follows. The descriptions of sample preparation, fluorescence up-conversion and RR setups, experimental conditions, and the procedures for data analysis are presented in the Experimental Section. The results from time- and frequency-domain measurements, DFT, and ab initio MO calculations together with correlations between time- and frequency-domain observations and the proposed photoisomerization model are presented in separate subsections in the results and discussion section. The main conclusions of this work are summarized in the conclusion section.

Experimental Section

Materials. Native PYP and its seven site-directed mutants (E46Q, T50V, R52Q, P68A, E46Q/T50V, E46Q/R52Q, and W119G) were prepared as reported previously.[4,6] Briefly, apo-PYP of *Ectothiorhodospira halophila* was heterologously overexpressed by *Escherichia coli*, followed by extraction with 8 M urea. Holo-PYP was then reconstituted in 4 M urea by adding *p*-coumaric anhydride.[4] It was purified with DEAE-Sepharose column chromatography (Pharmacia) and ammonium sulfate precipitation. The final buffer composition was 10 mM Tris-HCl and 1 mM PMSF (phenyl-methanesulfonyl fluoride) at pH

CHART 1. Structural Formulas of (a) the Native PYP Chromophore, Its Analogue Compounds (b) Caffeic Acid, (c) Dmac Acid, (d) Ferulic Acid, and (e) Locked Chromophore Used in This Work

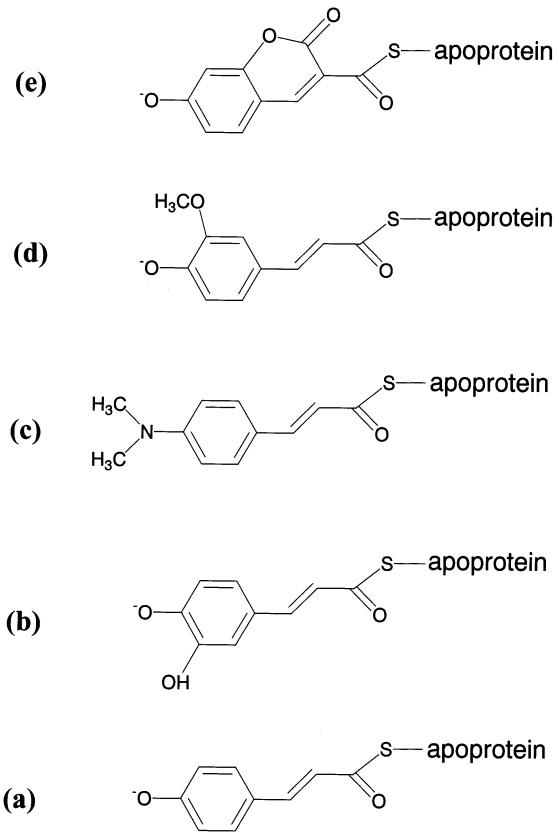

7.4. The optical purity index (abs at 277 nm/abs at 446 nm) for native PYP was ~0.45, and the absorbance at 446 nm was ~0.95 at 1-mm light path length. Reconstitutions of four PYP analogues (Chart 1) (7-hydroxy-coumarin-3-carboxylic acid, 3-methoxy-4-hydroxy-cinnamic acid, 4-dimethyl amino cinnamic acid and 3,4-dihydroxy cinnamic acid (hereafter abbreviated as locked chromophore, ferulic acid, dmac acid, and caffeic acid, respectively)) were carried out in the same manner as described by Imamoto et al.[4] Two PYP isotopomers, where the carbonyl carbon atom (C9) (denoted hereafter as $^{13}C{=}O$) or ring carbon atoms (C1−C6) (denoted hereafter as $^{13}C_6$-ring) of the chromophore were labeled with ^{13}C, have been prepared according to the methods described elsewhere.[4,39,44] For subsequent experiments, PYP was denatured by addition of 4 M guanidinium hydrochloride (GdnHCl) at pH ≈ 9.1, resulting in an unfolding of the protein and exposure of its deprotonated chromophore to water environment.

Fluorescence Up-Conversion Technique. The femtosecond time-resolved fluorescence decay curves were measured using a fluorescence up-conversion apparatus. A Ti−Sapphire laser system (Verdi-V8 pumped Mira 900, Coherent, Inc.) was used as a light source (120 fs, 76 MHz, 800 mW at 820 nm). The pulses were further compressed up to ~65 fs full width at half maximum (fwhm) using a prism pair compressor. The second harmonic (20 mW) was generated in a 0.1 mm thin BBO crystal and focused onto the sample, circulating in a flow cell (50 mL/min) with 0.5-mm light path length, to generate the fluorescence. It was collected with a pair of parabolic mirrors and focused together with the residual fundamental laser pulse on a 0.2-mm BBO type I crystal to generate the up-converted signal at the sum frequency. After the signal passed through a grating monochromator (1200 g/mm, Acton Research Corp.), it was detected by a photomultiplier (R1527P) coupled with a photon counter (C5410) system (both from Hamamatsu Photonics K. K.). The fluorescence decay curves were obtained by varying the optical path length of the delay stage for the fundamental laser pulse. Ten scans (with 6.67-fs steps) in alternate directions were accumulated to give a single transient with acceptable signal−noise ratio. As an instrument response function, a cross-correlation signal between fundamental and its second harmonic pulses was used (fwhm ≈ 110 fs). All measurements were carried out at room temperature (~20 °C). In these experiments, the optical density per 1-cm path length of PYP was 4−5 at 410 nm. By monitoring the steady-state absorption and fluorescence spectra before and after the scans, no degradation effects in PYP solutions were observed.

Low-Frequency RR Spectroscopy. RR spectra were obtained as described previously.[34] Briefly, a liquid nitrogen cooled CCD detector recorded the RR spectra after a Triax190 spectrometer (both from Instrument S. A., Inc.) removed the excitation light and a Spex 500M spectrometer (1800 grooves/mm grating, 0.5-m focal length) dispersed the scattered light. The 413.1- or 406.7-nm line from a krypton ion laser (BeamLok 2065, Spectra-Physics Lasers, Inc.) excited the samples at a 90° angle relative to the axis of the collection optics. A polarization scrambler was placed at the entrance of the spectrometer. All spectra were taken at room temperature (~23 °C), and a homemade software eliminated the noise spikes in the spectra caused by cosmic rays. The measurements were made on samples contained in a quartz-spinning cell (10 mm in diameter), and a rotation speed of 800 rpm was used. Measurements on PYP_{dark} were performed utilizing a low laser power (0.23 mW), while higher laser power (9.3 mW) was used for PYP_L.[45] Briefly, the lifetimes of the photocycle intermediates preceding the PYP_L are shorter than those of the PYP_L by more than 50-fold[9] so that their populations are negligible under the present experimental conditions.[34] RR spectra of PYP_L were obtained by subtracting a fraction of the normalized low-power spectrum from the normalized high-power one such that the $\nu_{11} = 1631$ cm^{-1} mode of PYP_{dark} (carbonyl C=O stretching mode of the chromophore) disappeared without introducing spurious derivative band shapes or negative peaks. An RR spectrum of fenchone was used as a calibration standard in the present study. A clear observation of its 96-cm^{-1} Raman band indicates that the present apparatus setup is capable of measuring signals down up to sub-100-cm^{-1} spectral region.

Computational Methods and Data Analysis. All analyses of fluorescence decay curves including the convolution of the model function (see below) with instrumental response were performed using Igor Pro graphics software (Version 3.1, WaveMetrics, Inc.). The quality of the fits (nonlinear least-squares fitting routine) has been judged by the χ^2 values (typically in order of 0.01) and the structureless distribution of fitting residuals around the zero for individual fits (see examples in Figure 3). Additional details concerning the absolute time-zero point estimation for individual transients in a broad spectral region can be found in our recent work.[20] Fourier transforms of individual decays were performed using the fast Fourier transform (FFT) algorithm to compute discrete Fourier transform spectra (DFTS). A Hanning window of a type, $(1 - \cos(2x/(N - 1)))/2$, was used before the FFT to reduce the spectral leakage in DFTS. The DFTS magnitudes were then adjusted for the lost energy due to windowing and scaled (for more details see Igor Pro User's Guide). The frequency resolution in these calculations was typically ±7 cm^{-1}. The bandwidths of the

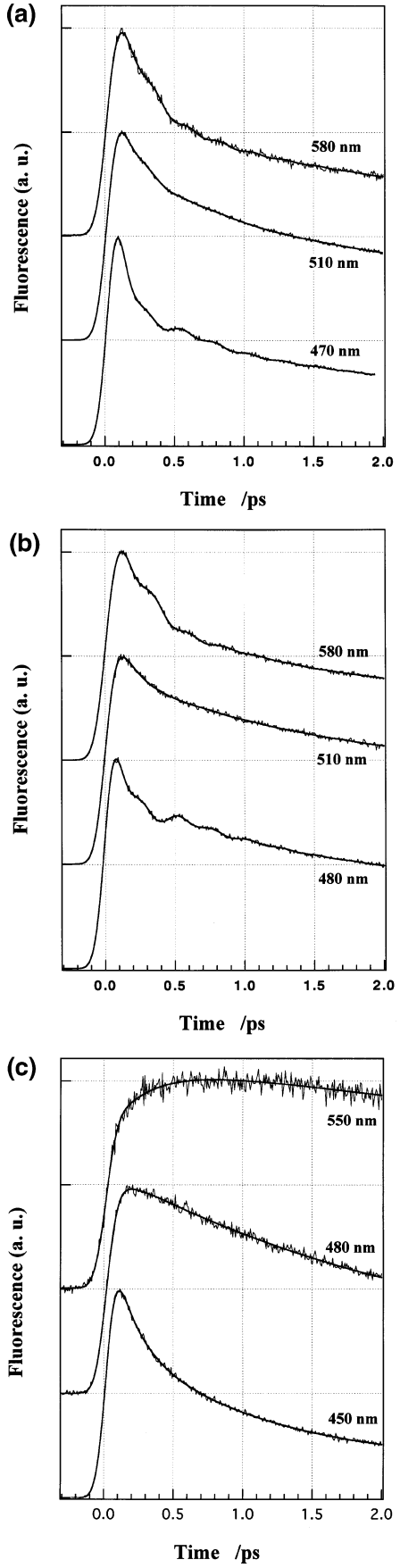

Figure 1. Fluorescence decay curves at three characteristic wavelengths on blue, top and red sides of the spectrum for (a) native PYP, (b) T50V mutant and (c) denatured PYP. The best fits obtained as a convolution of the *F(t)* function (eq 1) with the instrument response function are also shown (solid lines).

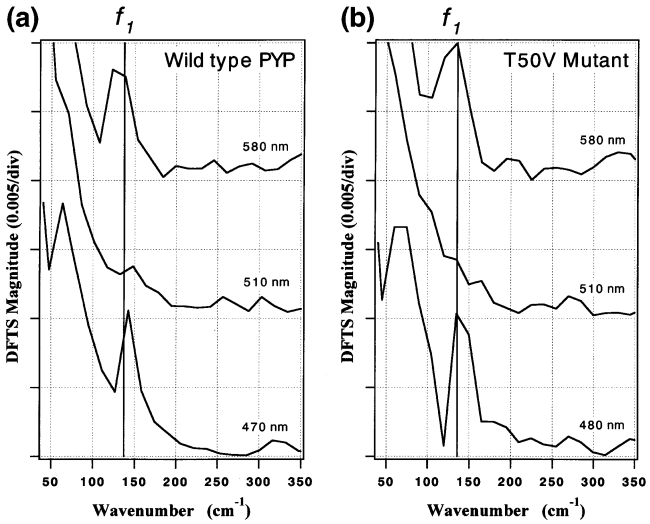

Figure 2. Low-frequency components in the fluorescence decays of (a) native PYP and (b) T50V mutant at three characteristic wavelengths on the blue, top, and red sides of the fluorescence spectra obtained by Fourier transformations.[49] The spectra were shifted by 0.01 step on the Ordinate axis for clarity. The reduction of the f_1 amplitude near the maximum wavelength (~510 nm) indicates that the process involving f_1 could be explained by transition frequency modulation mechanism. Concerning the f_2 mode, see the text. The spectral resolution of the Fourier transformations depends on the scan step (6.67 fs) and the number of points in the time-domain data set and is ± 7 cm^{-1} in the present analysis.

DFTS obtained by this procedure are not accurate and, hence, physically irrelevant.

The optimized geometry and harmonic vibrational frequencies for a chromophore model, deprotonated *trans*-4-hydroxycinnamyl ethyl thiolester (HCET), and locked chromophore analogue model, deprotonated 7-hydroxy-coumarin-3-carboxyl ethyl thiolester (HCCET), were estimated using various quantum chemical calculations.[46] Namely, Hartree−Fock (HF) and DFT using the 6-31G** basis set were used for the ground state (S_0), whereas the single-excitation configuration interaction (CIS) method with the 6-31G** basis set was employed for the excited-state (S_1) normal-mode calculations. These calculations were done using the Gaussian98 software package.[47] The hybrid functional B3LYP was used for the DFT calculations. No scaling factors have been used for calculated Raman frequencies since it is presumed not to be sensitive for low-frequency modes.

Results and Discussion

Local PNS Structure of PYP Mutants. Prior to presenting the main results of this study, we would like to recall in brief qualitative terms the specific changes in local PNS structure induced by site-directed mutagenesis. In the P68A mutant, the rigid proline group (Pro68) next to the binding site cysteine (Cys69) was replaced by the flexible alanine (Ala) group. This mutation does not perturb the hydrogen-bonding network around the phenolate anion ring of the chromophore, and its absorption peak and shape are almost identical with that of the native PYP. This mutation, however, considerably slows the fluorescence decay and implies that the weakening or loss of the rigidity of the PNS structure near the binding site of the chromophore makes the intrachromophore twisting reaction slower. In W119G, the tryptophane group (Trp119) far from the binding site of the chromophore was replaced by glycine (Gly). This mutation does not perturb the local PNS structure at all, and its absorption spectrum and primary photodynamics are identical to those of the native PYP. In E46Q, the glutamic acid group

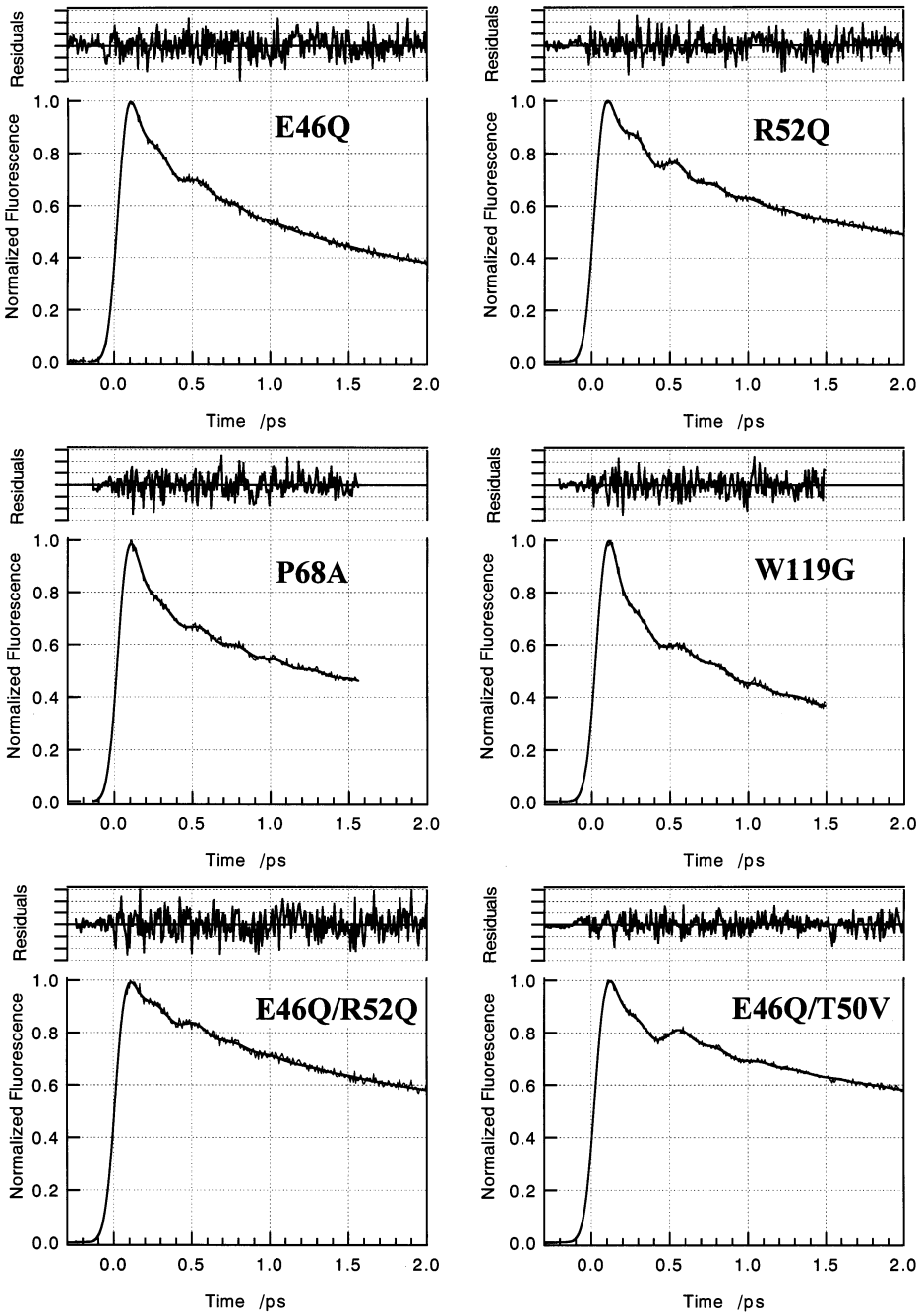

Figure 3. Examples of observed fluorescence decays at the blue edge of corresponding steady-state spectra with best fits and fitting residuals (upper panels, 0.01/div) for several site-directed mutants.

(Glu46) was replaced by glutamin (Gln). The hydrogen-bonding interaction between the NH_2 group of Gln46 and the O^- group of the phenolate ion is weakened compared with the native PYP, and the absorption spectrum of this mutant undergoes redshift by ~682 cm^{-1} (from 446 to 460 nm), probably due to the enhanced charge transfer (CT) from the O^- group to the other part of the chromophore caused by the weakening of the hydrogen-bonding interaction. In T50V, the threonine group (Thr50) was replaced by valine (Val). Though the Thr50 does not make a direct hydrogen bond with the O^- group of the phenolate ring, it makes a bond with tyrosine (Tyr42), which itself is hydrogen-bonded to the O^- of the chromophore; i.e., threonine stabilizes the overall hydrogen-bonding network in the PNS. Hence, the Thr50 → Val mutation effectively disturbs the hydrogen-bonding network and also weakens the Tyr42···O^- hydrogen bond, resulting in a ~540-cm^{-1} redshift of the absorption maximum of this mutant to 457 nm. Again, this redshift can be attributed to the enhanced CT in the chromophore. In the R52Q mutant, the positively charged arginine residue (Arg52) was replaced by neutral glutamin (Gln). Interestingly, the removal of the positive charge from the PNS almost does not affect the absorption spectrum of this mutant. This indicates that the positive charge on Arg52 plays a negligible role in the ground state of the protein. However, as we have shown by transient fluorescence measurements,[15] its absence in R52Q mutant considerably slows the photoisomerization dynamics of the chromophore in the excited state. In the case of the double mutants E46Q/T50V and E46Q/R52Q, the changes are as given for corresponding single mutants. Their absorption spectra are redshifted by ~1280 cm^{-1} (to 473 nm) and ~730 cm^{-1} (to 461 nm), respectively, and primary photodynamics are considerably slowed compared with that of the

native PYP. The steady-state absorption/emission spectra and more detailed descriptions of these mutants can be found in our previous works[14,15,18,20] and references therein.

Time-Domain Fluorescence Spectroscopy of Native and Mutant PYPs. Fluorescence decay dynamics of native PYP and related systems described in the Experimental Section have been measured at equidistant (10-nm step) wavelengths in a broad spectral region (460−620 nm), covering whole steady-state fluorescence spectra. Because the observed dynamics for native PYP as well as all mutants under investigation were qualitatively rather similar, only the results for the native PYP and T50V mutant at three characteristic wavelengths on the blue, top, and red sides of the spectrum in comparison with denatured PYP dynamics are shown in Figure 1. For intact proteins (parts a and b of Figure 1), the fluorescence decay curves with coupled oscillations can be well reproduced by the model function $F(t)$ convoluted with the instrument response

$$F(t) = \text{const} + \sum_i a_i \exp(-t/\tau_i) + \sum_j b_j \exp(-t/\tau_j^{\mathrm{d}})\sin(\varphi_j + \omega_j t) \quad (1)$$

Here $\omega_j = 2\pi f_j$ is the angular frequency of the jth mode, φ_j is the initial phase, and τ_j^{d} is the damping time of the jth mode. The analysis shows that the best fits could be reached when i and $j = 2$, i.e., double exponential decays superimposed with exponentially damping two oscillatory modes. On the other hand, for denatured PYP, no oscillations in fluorescence decays have been observed. The dynamics is dominated by *solvation effect*, i.e., faster initial decay at shorter wavelengths and corresponding rise at longer wavelengths. A three-exponential model function with a rise component was sufficient to reproduce accurately the dynamics in this case (Figure 1c). Before further discussions of the origins of oscillatory modes observed in fluorescence dynamics of intact proteins, we briefly note that two explanations for the nonoscillating dynamics behavior of denatured PYP are plausible, both clearly emphasizing the important role of the protein nanospace (PNS) as an environment for efficient photoreactions. First, if the oscillatory modes are of intrachromophore origin, they will be completely damped in denatured PYP owing to fast energy dissipation due to the interaction with surrounding water molecules. Second, if the vibrations originate from the chromophore−apoprotein interactions due to the hydrogen-bonding network in PNS, the chromophore exposure to water solvent (completely disordered state) will again cause the loss of coherence and natural disappearance of vibrations.

Let us now closely examine the oscillatory fluorescence dynamics of native PYP and T50V mutant (parts a and b of Figure 1). Some general features observed are described below. Although the photoinduced twisting of the chromophore in the mutant occurs as well, it is considerably slowed compared with that of the native PYP, emphasizing the optimal structure of the native PNS for the ultrafast and highly efficient photoreaction.[15,20] The twisting reactions in both cases occur immediately (within the time resolution of present measurements) after the ultrafast conversion from excited FC state to *vibrationally unrelaxed* Fl state. Furthermore, a spectral sharpening effect in the time domain, i.e., faster overall decays of fluorescence intensity on both the blue and red edges of the steady state spectra for both native and mutant PYP, is clearly observed.[15,20] Finally, two oscillatory modes coupled with the twisting reaction of the chromophore can be identified, a 135 ± 2-cm^{-1} underdamped mode (hereafter referred as f_1 mode) and a 50 ± 5-cm^{-1} overdamped mode (hereafter referred as f_2 mode) for the native PYP and 132 ± 2- and 63 ± 4-cm^{-1} modes for the T50V mutant, respectively. The fact that the amplitudes of both modes in T50V (also in other mutants at T50 position) are larger whereas the damping times are shorter compared with that of the native PYP suggests a major role for threonine in stabilizing the hydrogen-bonding network structure in PNS.

Two mechanisms could possibly contribute to the observed coherent oscillations in the spontaneous fluorescence. One is the modulation of the transition frequency (wave-packet motion on the excited-state potential surface), and the other is modulation of the mean transition dipole moment by the vibration (modulation of the fluorescence intensity). Interestingly, the wavelength-dependence behavior of the initial phase at "zero" time for these two mechanisms is different. While for the first mechanism a phase shift of π from "blue" to "red" (relative to the fluorescence maximum) is expected, there is no wavelength dependence in the second mechanism. Our analysis shows that the initial phases of the oscillatory modes depend on observation wavelength, and a phase shift of $\sim\pi$ from "blue" to "red" is clearly observed for both modes.[20] Hence, the observed coherent oscillations could be explained by the transition frequency modulation mechanism.[48] Further evidence supporting this mechanism is the fact that the amplitudes of vibrations are rather small at the maximum compared with those at the blue and red edges of the fluorescence spectrum. We should note that the oscillation frequencies were the same at all other monitored wavelengths except near the fluorescence maximum. Theoretically, at the wavelengths near the fluorescence maximum, a two times higher frequency is expected to be involved as a wave packet passes the maximum of the spectrum twice in one period. Practically, however, the amplitude of the "double" frequency is expected to be rather small due to a broad fluorescence spectrum and finite time/frequency resolution. Furthermore, in our experiments, the bandwidth we can excite impulsively is estimated to be ∼175 cm^{-1} (∼90 fs at 410 nm), i.e., not enough to capture the expected double mode at around ∼270 cm^{-1}. The described pattern with no oscillating component at the fluorescence maximum is clearly observed for the f_1 mode in Fourier transformations of decays presented in Figure 2.[49] On the other hand, for the f_2 mode, the picture is a little complicated. The expected double frequency near the fluorescence maximum is not clearly seen though the applied time resolution should have been able to resolve it. At present, we can only speculate that its overdamped nature due to strong coupling with the environmental protein in PNS and/or the possible presence of another mechanism(s) are the reasons for this discrepancy. We stress that the trivial possibility for the f_2 mode of being an experimental artifact is excluded because its existence was accurately verified with repeated comparative experiments (including also porphyrins[50] and another family of proteins such as flavoproteins showing no oscillations).[51]

The general features in other mutants examined in this work are qualitatively rather similar to the above-described picture, and similar oscillatory modes (130−140 cm^{-1} and 40−70 cm^{-1}) have been observed as well. Some decay examples are presented in Figure 3. On the basis of the data summarized in Table 1, we conclude that the frequency of the underdamped f_1 mode and its coupling to the electronic excited state does not change dramatically due to the mutation though the damping time tends to decrease slightly as the PNS structure becomes looser and more disordered by mutation. This is a strong indication for the f_1 mode being of an intrachromophore origin because, in

TABLE 1: Oscillation Frequencies Coupled with the Spontaneous Fluorescence Decay Dynamics for Native PYP and Its Seven Mutants

	native PYP	W119G	E46Q	R52Q	P68A	T50V	E46Q/T50V	E46Q/R52Q
f_1 (cm^{-1})	135 ± 2	133 ± 2	135 ± 4	137 ± 2	138 ± 2	132 ± 2	130 ± 2	133 ± 5
f_2 (cm^{-1})	50 ± 5	55 ± 8	66 ± 8	69 ± 8	48 ± 15	63 ± 4	58 ± 3	75 ± 22

contrast to intermolecular (chromophore-protein) modes, the frequencies of intrachromophore modes are expected to be lesser affected by the protein environment. For the f_2 mode, the relative spread of frequencies depending on mutation is larger compared with the f_1 mode and its damping time considerably decreases as PNS becomes more disordered by mutation. Hence, we speculate that it is due to some intrachromophore low-frequency vibration sensitively "feeling" weak chromophore−protein environment interactions and its damping time corresponds probably to fast dephasing rather than to relaxation. Although an accurate quantitative analysis of damping times for each coupled mode in correlation with a specific mutation site would be most desirable, such an analysis at this stage is hampered by the time resolution of present experiments and methods/models used to subtract off the underlying nonexponential decays.

Analogue PYPs. Another way to gain further insight into the primary dynamics of PYP is to study PYP analogues with modified chromophores.[20] This has attractive features because various kinds of small substituents can be attached to different positions of the chromophore with an aim of studying their effects on PYP dynamics while not much disturbing the overall structure of the protein.[52] The replacement of the native chromophore with a modified one may induce specific changes in the chromophore, such as an amino acid residue hydrogen-bonding network, resulting in a more or less perturbed overall structure of the PNS. Four such hybrids with ferulic acid, dmac acid, caffeic acid, and locked chromophores have been investigated. Static UV−vis spectroscopy of these analogues suggests that their structures are not drastically disturbed, yet as we have found recently, their primary dynamics qualitatively differ from those of native as well as mutant PYPs.[14,15,18−20] Fluorescence dynamics of ferulic acid, dmac acid, and caffeic acid analogues show the familiar picture of *solvation dynamics* qualitatively resembling that of the denatured PYP (Figure 1c), whereas the oscillations are almost negligible.[19,20] These observations strongly suggest that the PNS of these analogues are disordered. When these hybrids are excited, a strong intrachromophore charge transfer from substituents to the phenyl ring and further to the thioester bond takes place instantaneously.[20] The large dipole moment of the excited chromophore strongly interacts with nearby amino acid residues undergoing ultrafast stabilization in the disordered PNS, demonstrating the ultrafast dynamic Stokes shift of fluorescence.[20] This behavior was actually expected because the reorganization energy associated with the photoexcitation and fluorescence emission (Stokes shift) in these systems is fairly larger (∼3030, 3060, and 3230 cm^{-1}, respectively) compared with that of native PYP (∼2180 cm^{-1}). For comparison, we note that in all mutants examined the Stokes shift is equal or smaller than that of native PYP and no solvation effect was observed in these systems.[15] Because in these three analogues the vibrational couplings with spontaneous fluorescence are very weak, we do not present further discussions here. Details concerning these observations and quantitative analysis of solvation time correlation function $C(t)$,[54] characterizing in this particular case the intraprotein amino acid reorientation times, are presented in our recent paper.[20] It was also demonstrated that the solvation time of the excited chromophore in PNS of the ferulic acid analogue is by far shorter than that of the denatured PYP.[20] These results together with the considerably redshifted absorption spectra of these analogues[53] (compared with those of the denatured PYP) seem to give a confirmation that the observed phenomena are of *intraprotein* origin.

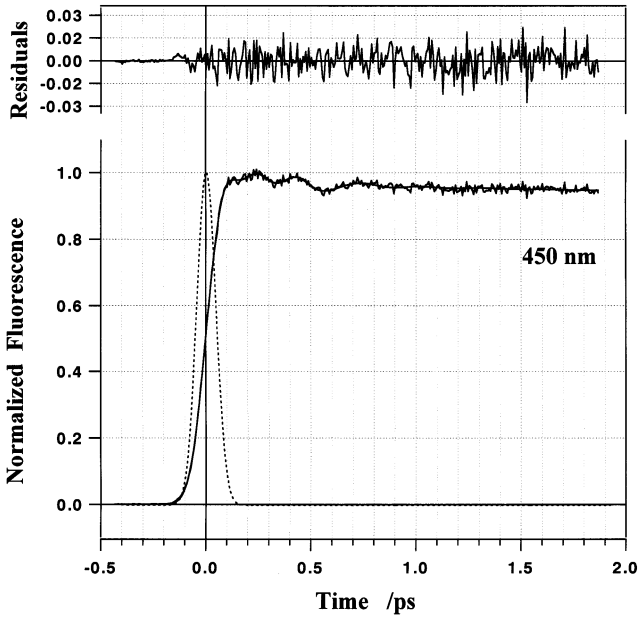

Figure 4. An example of fluorescence decay for the locked chromophore analogue at the blue edge of the steady-state spectrum. The best fit (solid line) obtained as a convolution of the $F(t)$ function (eq 1) (one-exponential decay (∼60 ps) and three oscillating components) with the instrumental response (dashed line) is also shown. The upper panel shows fitting residuals.

On the other hand, fluorescence dynamics of the PYP analogue with locked chromophore is of primary interest. Its absorption at ∼443 nm and rather small Stokes shift (∼1100 cm^{-1}) indicate that the chromophore is not exposed to a water environment being well accommodated in the PNS, and no solvation effect in its primary dynamics was observed.[20] In this analogue, the vinyl double bond of the chromophore is locked by the presence of a covalent bridge over the vinyl bond; i.e., the twisting motion around the double bond and also the flipping of the thiolester linkage are hampered. As expected, the fast femtosecond and picosecond components totally disappear and the fluorescence decay becomes very slow (∼60 ps),[13,20] indicating that the ultrafast photoisomerization does not occur at all. This observation nicely shows the ability of transient fluorescence spectroscopy in "visualizing" the correlation between the chromophore structure and its photoisomerization rate. Furthermore, weak oscillatory features on both short- and long-wavelength regions of the locked chromophore analogue spectrum could be observed.[20] It was not possible to reproduce the decay profiles with two oscillatory components in analogy with those of native PYP, however, a model function with three oscillatory components could nicely fit the experimental decays. A decay example is shown in Figure 4. The fits predict the frequencies of coupled oscillatory modes for the locked chromophore analogue to be ∼60, 115, and 165 cm^{-1}. For convenience, further analysis and comparative discussions concerning the frequencies of coupled modes in different systems

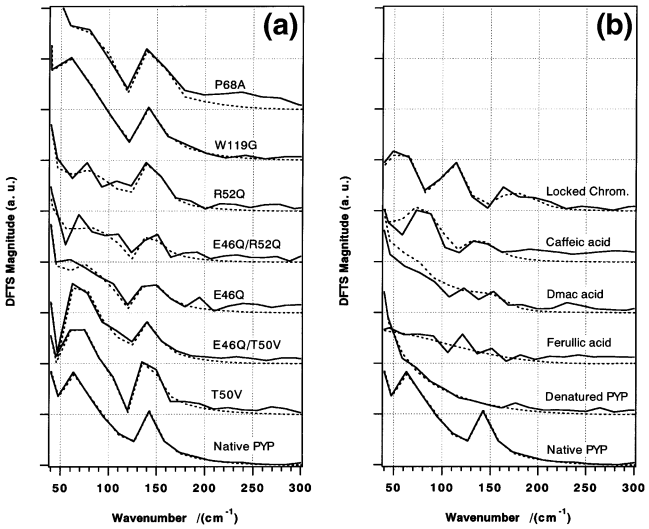

Figure 5. Frequency components in the fluorescence decays at the blue edge of the steady-state fluorescence spectra of (a) native PYP and its mutants and (b) denatured PYP and four-analogue systems obtained by Fourier transformation.[49] The solid lines are Fourier transforms of experimental data and dashed lines are Fourier transforms of the fits in "time" space. The spectral resolution depends on the scan step (6.67 fs) and the number of points in the time-domain data set, and is ± 7 cm^{-1} in this case. The spectra were shifted by a 0.01 step on the Ordinate axis for clarity.

are hereafter carried out in the frequency-domain representation presented below.

DFTS Representation and Analysis. In Figure 5, DFTS of time-domain experiments for (a) native PYP and its seven mutants and (b) native PYP, denatured PYP, and four analogue systems are summarized. Though the spectral resolution of these transformations is low (± 7 cm^{-1}), it is a visually easy and rather reliable way for qualitative comparison of the low-frequency modes coupled with the transient fluorescence for different systems and also with low-frequency RR spectra. In denatured PYP, there are no detectable vibrational modes. The heavy background at the low-frequency region is due to the fast exponential decay in the time space. In native PYP and all mutants, there are two dominant modes involved ($\sim$60 and 140 cm^{-1}). It is interesting to note that, for W119G, where the tryptophane/glycine mutation is located far from the binding site of the chromophore, the transient fluorescence and also the DFTS spectrum are almost identical with that of native PYP. This observation directly confirms the hypothesis that primary photophysical processes in PYP are controlled exclusively by the PNS.[15,20] On the other hand, in the E46Q mutant, where the glutamic acid/glutamin mutation perturbs (presumably weakens)[55] the hydrogen bond with O^- of the chromophore, the amplitude of the 140-cm^{-1} mode is reduced approximately by two times compared with the native one. This would qualitatively agree with the low-frequency RR observation (undetectable 153 cm^{-1} mode, see below). In all these mutants, a flipping and consequent isomerization of the chromophore occurs with a little longer time constants compared with the native one and no big qualitative differences are seen on the ultrafast time scale. However, in PYP analogues, the picture is rather different and intriguing. For ferulic acid analogue, the vibrations are almost negligible. If there is a coupled vibrational mode at all, it should be at around 120 cm^{-1}. Recently we have shown that in this analogue system a strong "intraprotein solvation" effect is also present,[20] so it is really difficult to determine from transient fluorescence experiments alone if a photoisomerization reaction occurs at all. A qualitatively similar picture prevails also for the dmac acid analogue. For the caffeic acid analogue, when the chromophore is modified at the C6 position by an $^-$OH group (comparatively smaller distortion compared with those of ferulic and dmac acid analogues, Chart 1), the DFTS is somewhat similar to the native PYP but with a little shifted modes and nearly two times reduced magnitudes. On the other hand, in the case of the locked chromophore analogue with no detectable solvation effect, one can clearly see two modes at around 115 and 165 cm^{-1} instead of a single mode at $\sim$135 cm^{-1} observed for the native protein. While in the locked chromophore analogue a fast photoisomerization reaction does not occur at all,[13,20] it is reasonable to speculate that the observed difference in DFTS in one or another way is related to it. Hence, detailed comparative analysis of low-frequency RR spectra of native PYP and the locked chromophore analogue will surely shed more light on the nature and role of coherently coupled vibrational modes in photoisomerization reaction dynamics of PYP and related systems.

As described in the Experimental Section, the spectral range of the present RR experiments does not cover the f_2 ($\sim$50 cm^{-1}) mode, making its comparative analysis in time and frequency domains based only on DFT calculations. In the following, this mode will be discussed only in brief terms where possible and hereafter we will mainly concentrate on the origin and role of the underdamped f_1 mode.

Frequency-Domain RR Spectroscopy. Low-frequency RR spectra of the calibration standard (neat fenchone), PYP_{dark}, PYP_L, and denatured PYP are shown in Figure 6. Denatured PYP did not show any significant low-frequency Raman bands. Presumably, the exposure of the chromophore to the water environment (disordered state) results in complete suppressing of intrachromophore normal modes. One of the possible explanations could be the large inhomogeneous broadening of the Raman bands. Low-frequency modes are likely to be strongly coupled with protein vibrations. Thus, disordered protein structures with different chromophore−protein vibrational couplings could lead to significantly broad and experimentally not observable low-frequency Raman bands. This is in full agreement with nonoscillating fluorescence dynamics in time-domain experiments described above. This observation also emphasizes the importance of the PNS environment in "preserving" the normal modes even in the ground state. In the 100−210-cm^{-1} spectral region, there are at least four Raman bands for PYP_{dark} at 104, 153, 183, and 202 cm^{-1}. Although the relative intensity of the 104-cm^{-1} band is rather small ($\sim$10%), it was clearly observed in the higher power spectrum (not shown), where both PYP_{dark} and PYP_L are present. The Raman band at 153 cm^{-1} seems to be a singlet, while bands at 183 and 202 cm^{-1} are observed as poorly resolved doublets. For PYP_L, only one band at 191 cm^{-1} can be clearly distinguished in the same spectral region within present S/N ratio. At this stage, it is not clear whether the other features around 100−150 cm^{-1} represent a real signal or not. Presumably, drastic spectral differences observed for PYP_{dark} and PYP_L in the whole 100−800-cm^{-1} region arise from the structural alterations in the chromophore (complete trans/cis isomerization) and its vicinity (broken and/or regrouped hydrogen bonds) due to the photoconversion from PYP_{dark} to PYP_L. In contrast, the changes observed in 800−1600-cm^{-1} spectral region were relatively moderate.[34] This can be attributed to the fact that below 800 cm^{-1}, normal modes of the *chromophore skeleton*, which are usually more sensitive to the intrachromophore and/or PNS structural changes, start to appear. A complete assignment of the low-frequency bands and characterization of observed

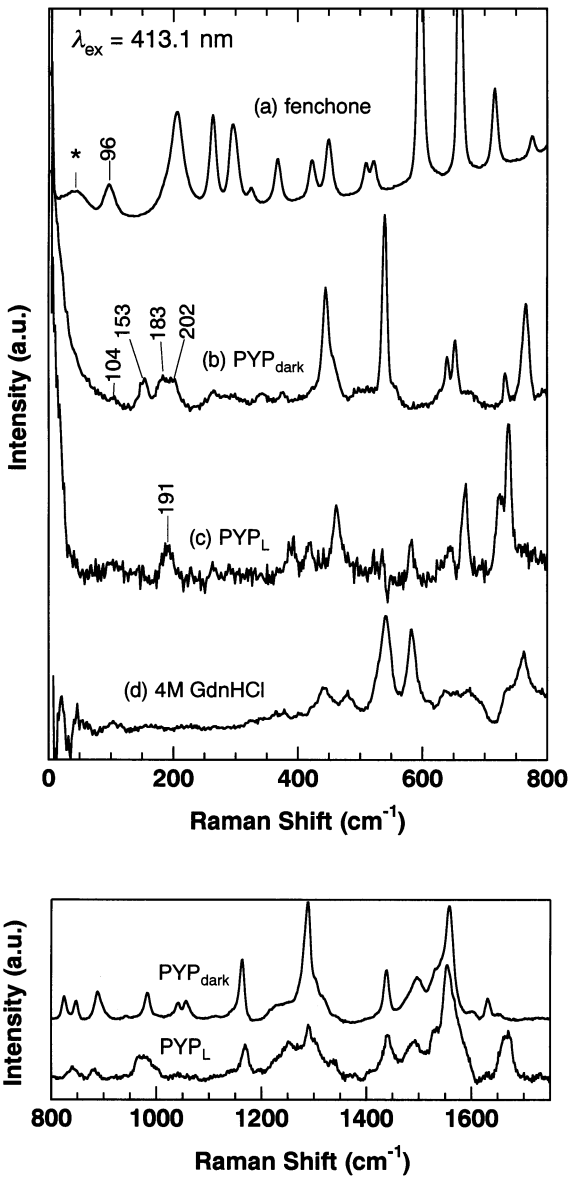

Figure 6. Upper panel: Low-frequency RR spectrum of the (a) calibration standard fenchone and RR spectra of (b) native PYP_{dark}, (c) PYP_L, and (d) denatured PYP. Note that in part a the lower frequency band at around 50 cm^{-1} (marked with an asterisk) is due to an experimental artifact. Lower panel: RR spectra of PYP_{dark} and PYP_L in the 800−1750-cm^{-1} spectral region.

differences for PYP_{dark} (referred hereafter as PYP for simplicity) and PYP_L is not in the scope of this paper and will be addressed in a future work. In the following, we will explore only the 100−210-cm^{-1} region with an aim to find correlations with time-domain observations.

On the other hand, the two isotopically labeled samples did not show any remarkable spectral changes compared with those of native PYP (data not shown). Generally, in a higher-frequency spectral region, isotope effects usually cause a few wavenumber shifts of corresponding Raman bands of a labeled site or bond effectively identifying them. However, in the low-frequency region, skeletal vibrations of the chromophore as a whole give rise to the low-frequency modes, making the expected isotope shifts for chromophore isotopomers smaller. Our DFT calculations predict that the expected isotope shifts of the low-frequency modes for both examined isotopomers are within 2 cm^{-1}. In the present experiments, the shifts were indeed within 2 cm^{-1}, however, a rigorous error analysis indicated that the fitting error

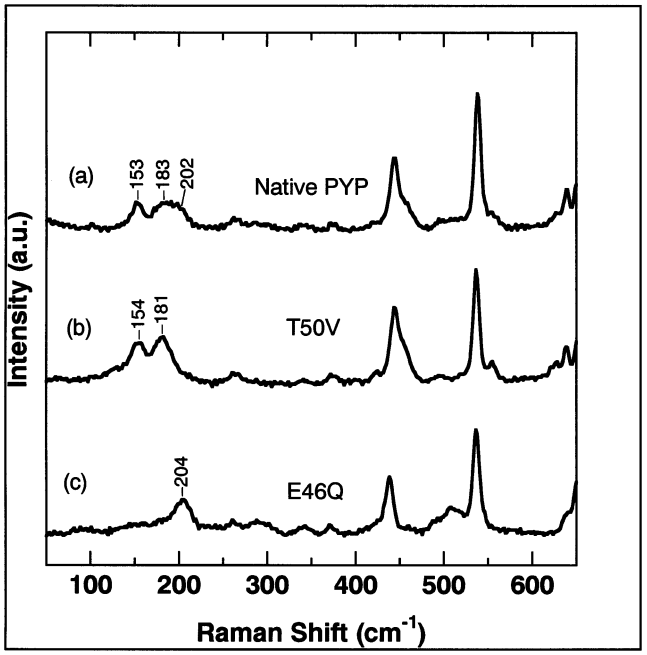

Figure 7. Low-frequency RR spectra of (a) the native PYP, (b) T50V, and E46Q (c) mutants. Peak positions were obtained from fitting analysis using a multi-Gaussian with straight baseline model function.

is also about 1−2 cm^{-1}. Hence, we cannot use RR data for both isotopically labeled samples for *firm and unambiguous* assignments. However, if we dare to speculate that observed shifts are qualitatively real, they seem to be consistent with and support our tentative assignments based on observed and calculated frequencies and intensities (see below). In principle, for firm assignments, one could expect that designing and synthesizing new isotopomers with larger band shifts would solve the problem. However, our DFT calculations suggest that, even if all carbon atoms of the chromophore are replaced with ^{13}C, the expected isotope shifts will be still very small, a few wavenumbers. Thus, we think that the goal of the full assignment could be probably reached by using mutant and/or analogue compounds. In contrast to isotopomers, the spectral differences are more pronounced in site-directed mutants. Low-frequency RR spectra of two mutants E46Q and T50V together with those of native PYP are presented in Figure 7. In the case of the T50V mutant, the 153- and 183-cm^{-1} modes are almost unchanged while the intensity of the 202-cm^{-1} mode has been critically reduced. In the case of the E46Q mutant, an opposite tendency is observed; namely, intensities of both the 153- and 183-cm^{-1} modes are critically reduced while that of the 202 cm^{-1} has slightly increased and a little upshifted to 204 cm^{-1}. These drastic changes indicate that the low-frequency modes are strongly affected by the mutation; i.e., the low-frequency modes are highly sensitive to protein environment in contrast to high-frequency modes where no such dramatic effects were observed.[34,39,40] Evidently, these observations are connected with perturbations of an H-bonding network in both mutants, but tackling these effects is not an easy task, and at the present stage, we have no straightforward and complete explanation for the observations in mutants. At any rate, this is a very exciting finding and further investigations on low-frequency RR spectra of site-directed mutants are now in progress.

DFT and ab initio MO Calculations; Correlations between Time- and Frequency-Domain Observations. One should note that comparison of results from time- and frequency-domain experiments should be carried with some important precautions addressed in the following. In time-domain experiments, we are

observing the oscillations of the *spontaneous* fluorescence reflecting *only* the excited-state properties of the protein; hence, there is no question that the oscillations also originate from the excited electronic state of the protein (most probably a wavepacket motion on the excited-state potential surface). Contrary, RR spectroscopy probes the vibrational modes in the ground state coupled to *excitation* of the protein. Hence, (1) the time-resolved experiments described here *are not* time-domain analogues of RR, and Fourier transforms cannot be directly compared with it. Moreover, (2) not all modes in the excited state should be necessarily strongly coupled to electronic excitation of the protein and modulate its spontaneous deactivation; i.e., the number of vibrational modes observed in time-domain is usually less than the number of modes observed in RR in a given spectral region. (3) There could be large/significant structural rearrangements in PNS upon photoexcitation, which could alter and shift low-frequency modes in the excited state. Finally, (4) not all fundamental modes are necessarily Raman active in resonant-excitation conditions. These problems could be theoretically overcome by applying the time-resolved excited-state Raman spectroscopy technique.[56] However, our attempts to measure RR spectra of PYP's excited state or its transient photointermediate states were unsuccessful because of a rather strong fluorescence from the sample. On the other hand, model quantum mechanical calculations have proven to be a good way for normal modes estimation. In earlier works exploring the higher-frequency region of RR spectra, *trans*-4-hydroxycinnamyl methyl thiolester (HCMT) was successfully used as a model for PYP chromophore.[34,39,40] Similar calculations on HCMT were performed also for the low-frequency region. However, it was found that methyl group couples to low-frequency modes of the chromophore, especially for the important ~150-cm^{-1} mode and different degrees of coupling from methyl group to low-frequency modes of the chromophore, causes big discrepancies in HF and B3LYP calculations. Inclusion of the main-chain carbon atoms in the model could probably solve this problem. Hence, we replaced a terminal methyl group in HCMT with an ethyl group in HCET to include Cα of Cys69, and in the present calculations, HCET for native and HCCET for analogue PYP chromophores were used as models.[57] This choice of model chromophores, as stated above, is based on a precaution that truncation of a covalent bond between the chromophore and protein could potentially affect low-frequency modes.

Optimized structures and calculated atomic displacements for selected normal modes of HCET and HCCET are presented in Figure 8, and observed and calculated frequencies for native PYP and its model (*trans*-HCET) and locked chromophore analogue and its model (HCCET) are summarized in Table 2. The Raman bands in native PYP's spectrum at 183 and 202 cm^{-1} are assigned to in-plane skeleton-bending modes ν_{42} and ν_{41}, while the bands at 104 and 153 cm^{-1} are assigned to out-of-plane skeleton-bending modes γ_{17} and γ_{16}, respectively. Furthermore, a close examination of the computed frequencies in the ground S_0 (HF, B3LYP) and excited S_1 (CIS) states reveals that calculations predict a slight downshift tendency for the out-of-plane (γ) modes in the (excited) S_1 state whereas in-plane (ν) modes are almost unchanged in both (ground) S_0 and (excited) S_1 states. This result supports qualitatively the assignment of the f_1 (135 cm^{-1}) mode observed in time-domain fluorescence experiments to γ_{16} (130 cm^{-1} for CIS) because the RR spectrum of the native PYP shows a band at 153 cm^{-1} (146 cm^{-1} for DFT). Concerning the f_2 (~50 cm^{-1}) mode observed in time-domain experiments, the calculations predict two possibilities; i.e., it could be the ν_{43} or the γ_{18} mode. However, because the probability of out-of-plane modes involvement in the photoisomerization process is higher, we speculate that its assignment to the γ_{18} mode is more plausible.

TABLE 2: Observed and Calculated Frequencies (Normal Modes in Ground (S_0) and First Excited (S_1) States) for the Native PYP and Its Model *trans*-HCET and the Locked Chromophore Analogue and Its Model (HCCET)

fluorescence (S_1) ν_{obs}/cm^{-1}	Raman (S_0) ν_{obs}/cm^{-1}	HF (S_0) ν_{cal}/cm^{-1}	B3LYP (S_0) ν_{cal}/cm^{-1}	CIS (S_1) ν_{cal}/cm^{-1}	assignment[57]
		Native PYP			
		35	31	19	γ_{20}
		47	40	31	γ_{19}
		67	70	69	ν_{43}
50		81	55	63	γ_{18}
	104	106	81	101	γ_{17}
135	153	154	146	130	γ_{16}
	183	186	177	183	ν_{42}
	202	237	219	238	ν_{41}
		241	228	195	γ_{15}
		259	245	257	ν_{40}
		Locked Chromophore Analogue			
		32	29	25	γ'_{20}
60		61	58	59	γ'_{19}
115		102	90	106	ν'_{43}
		81	79	61	γ'_{18}
		118	115	95	γ'_{17}
165		185	177	149	γ'_{16}
		139	123	141	ν'_{42}
		216	207	215	ν'_{41}
		255	238	237	γ'_{15}
		240	225	241	ν'_{40}

We have tried to measure the low-frequency RR spectrum of the PYP analogue with locked chromophore at two excitation wavelengths (413.1 and 406.7 nm), but it revealed that in both experiments weak low-frequency Raman bands were obscured by a strong fluorescence from the sample (data not shown). The fluorescence quantum yield of the locked chromophore analogue was estimated to be ca. 0.09 (for comparison, the yields for native PYP, its chromophore model *trans*-pCA^{2-}, and ferulic acid analogue are ~10^{-3}, 3×10^{-3}, and 5.4×10^{-2}, respectively);[29,32,58] i.e., it is nearly 2 orders of magnitude larger compared with that of the native PYP, and this sample seems not to be suited for RR spectroscopy. Unfortunately, the non-RR experiments failed, too, because the Rayleigh scattering from the sample was too big to see small Raman bands. Other possibilities now in consideration are the anti-Stokes Raman spectroscopy and a nonresonance experiment on a crystalline or dried film sample where the amount of water is relatively small. At the present stage, however, we have to content ourselves with the discussion and assignments of the oscillatory modes observed for locked chromophore analogue in the time domain based only on the DFT calculations. The ~60-cm^{-1} mode of locked chromophore analogue (Table 2) could be either the γ'_{18} or the γ'_{19} mode (61 and 59 cm^{-1} in CIS calculations for HCCET, respectively). Similarly, the ~115-cm^{-1} mode could be correlated with γ'_{17} or ν'_{43}, and the ~165-cm^{-1} mode could be either the out-of-plane γ'_{16} or the in-plane ν'_{42} modes, respectively. However, because in the locked chromophore analogue the fast photoisomerization does not occur at all, one could speculate that both modes at 115 and 165 cm^{-1} are of in-plane origin; i.e., they correlate with the ν'_{43} and ν'_{42} modes, respectively. This hypothesis is indirectly supported also by the fact that the Stokes shift of the locked chromophore analogue is two times smaller compared with that of the native protein. In other words, in this analogue system, where the chro-

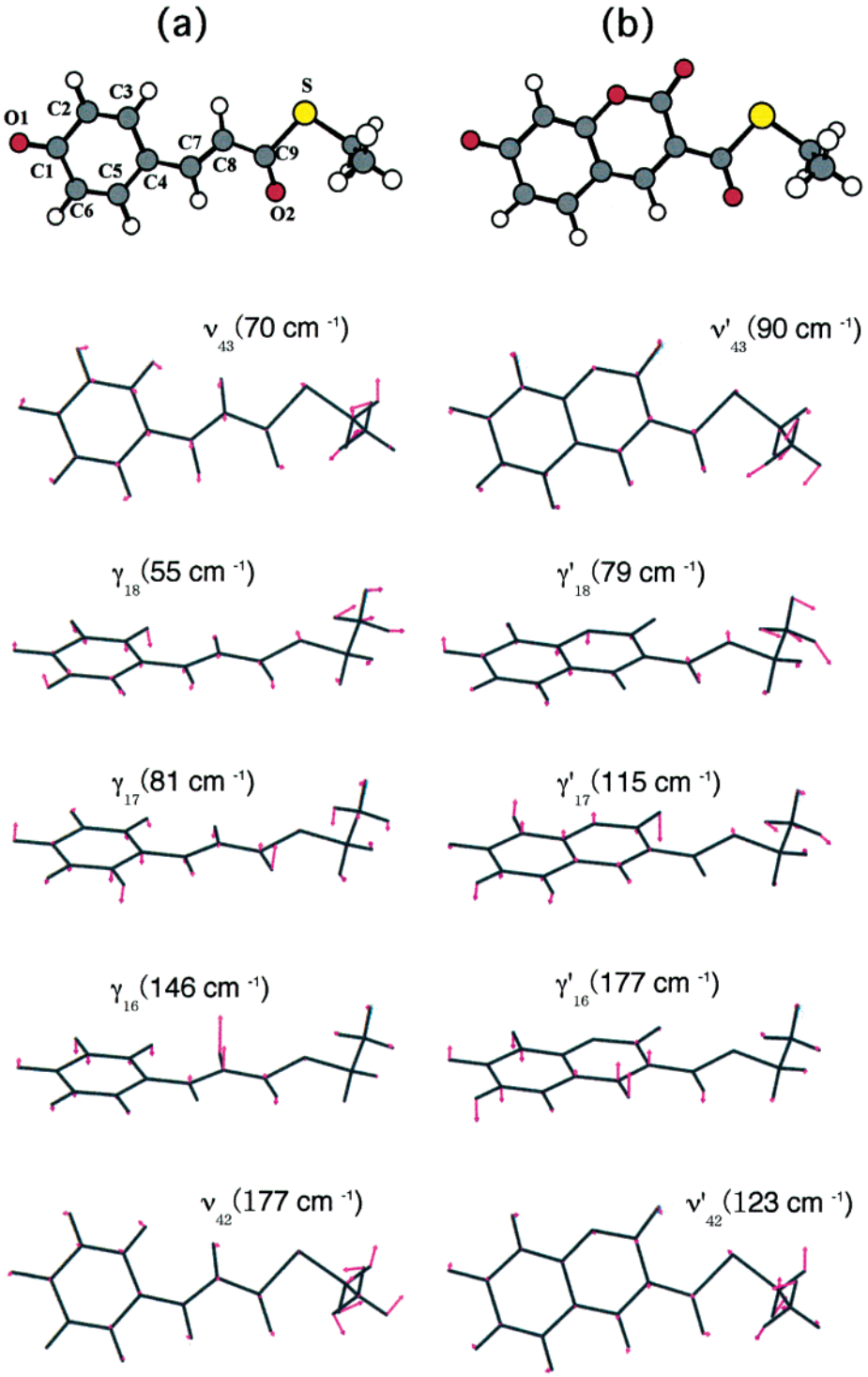

Figure 8. A sketch of the optimized structures for (a) *trans*-HCET and (b) HCCET and some selected low-frequency vibrational modes in the ground state. Arrows in each sketch show corresponding atomic displacement vectors. The frequency values obtained from DFT (B3LYP) calculations for presented modes are also given.

mophore's large scale out-of-plane movements, flipping, or twisting are unlikely due to its rigid structure, only totally symmetric A′ (in-plane) modes with no role in photoisomerization reaction couple to the transient fluorescence and are responsible for the observed oscillations. Nevertheless, the lowest mode (~60 cm^{-1}) observed in time-domain experiments, as we have already discussed for native and mutant PYPs, is more sensitive to the PNS structure (i.e., chromophore−apoprotein interactions). Hence, there is a possibility that this mode could have an out-of-plane origin also in locked chromophore analogue (γ'_{18} or γ'_{19}), because the stronger coupling to amino acid residues in PNS could activate corresponding A″ out-of-plane modes.[59]

We stress again that these assignments are based on the vibrational analysis of the chromohore alone, and in this regard present assignments are *tentative*. Further experimental studies are required for firm assignments. In calculations, one needs also to consider the effects of the PNS on the low-frequency modes. Hence, further DFT and ab initio MO calculations mimicking apoprotein−chromophore interactions by introducing intermolecular hydrogen bonds around HCET, steric, and/or electrostatic effects of the protein moiety, etc., may shed more

light on the RR spectra and help to obtain detailed structural information that cannot be easily derived from the experiments alone.

The "Trigger Mode Mediated Guidance" Photoisomerization Model for PYP. On the basis of the above presented results and analysis, here we present a possible photoisomerization model for PYP and call it "trigger mode mediated guidance". After a blue-light absorption, the system is elevated into the Franck−Condon excited electronic state with excess vibrational energy due to a number of intrachromophore vibrational modes. FC → Fl conversion takes place rapidly accompanied with ultrafast IVR leading to the Fl state with selectively excited coherent modes. One of these modes, identified as γ_{16}, manifests itself as oscillations in the fluorescence decay, flips the C8 carbon and corresponding hydrogen atoms of the chromophore (see corresponding atomic displacements of the γ_{16} mode in Figure 8), and effectively triggers the isomerization. Though the estimated energy of this mode is pretty low (150 $cm^{-1} \approx 0.5$ kcal/mol), it still may drive a portion of excited chromophores into the twisted state because the fastest process in PYP has been shown to be of a barrierless origin.[15] Because the mutation effect in time-resolved experiments almost does not affect this mode (Table 1), we suppose that it only triggers the reaction without controlling its rate. On the other hand, for the lowest mode ($\sim$50 cm^{-1}), the relative spread of frequencies depending on mutation was remarkably larger and its damping time considerably decreased as PNS becomes more disordered by mutation. Hence, we speculate that this mode could "guide" the twisting and probably control also the reaction rate. Finally, the nonuniform protein environment secures the unidirectionality of the photoisomerization; i.e., it explains why the isomerizable bond, once it reaches the transition state, does not return immediately to the trans conformation that perfectly matches the protein environment but instead forms the cis conformation, causing the mismatch with the protein environment that drives the rest of the light cycle. The essential difference between the proposed model and the model presented by Genick et al.[31] is the inclusion of the concept of the low-frequency coherent "trigger" and "guidance" modes into the reaction scheme. For quantitative confirmation of the proposed model, further dynamics studies using $\sim$30-fs time resolution as well as complete assignment of PYP's low-frequency vibrational modes are currently in progress.

Conclusions

In this work, a first attempt to disclose the origins and role of low-frequency vibrations in primary photodynamics of PYP has been done. The existence of two oscillating components in the time-resolved fluorescence decays, its intrachromophore origin, and the influence of the PNS environment onto these modes have been shown unambiguously for native and mutant PYP. Furthermore, low-frequency RR spectroscopic measurements have been performed on native PYP and its two mutants for the first time. Correlations between time- and frequency-domain experiments have been observed and discussed. Tentative assignments of low-frequency modes manifested also in the time-resolved fluorescence data have been made supported by DFT and ab initio MO calculations. A qualitative model has been proposed to explain in simple terms the ultrafast primary process initiating PYP's photocycle. For quantitative confirmation of the proposed model, additional experiments will be required.

Acknowledgment. The authors thank Dr. Y. Imamoto for providing site-directed mutants of PYP and helpful discussions.

References and Notes

(1) Meyer, T. E. *Biochim. Biophys. Acta* **1985**, *806*, 175.
(2) Hoff, W. D.; Dux, P.; Devreese, B.; Roodzant-Nugteren, I. M.; Crielaard, W.; Boelens, R.; Kaptain, R.; Van Beeumen, J.; Hellingwerf, K. J. *Biochemistry* **1994**, *33*, 13959.
(3) Baca, M.; Borgstahl, G. E. O.; Boissinot, M.; Burke, P. M.; Williams, D. R.; Slater, K. A.; Getzoff, E. D. *Biochemistry* **1994**, *33*, 14369.
(4) Imamoto, Y.; Ito, T.; Kataoka, M.; Tokunaga, F. *FEBS Lett.* **1995**, *374*, 157.
(5) Kort, R.; Hoff, W. D.; Van West, M.; Kroon, A. R.; Hoffer, S. M.; Vlieg, K. H.; Crielaard, W.; Van Beeumen, J.; Hellingwerf, K. J. *EMBO J.* **1996**, *15*, 3209.
(6) Mihara, K.; Hisatomi, O.; Imamoto, Y.; Kataoka, M.; Tokunaga, F. *J. Biochem.* **1997**, *121*, 876.
(7) Hoff, W. D.; van Stokkum, I. H. M.; van Ramesdonk, H. J.; van Brederode, M. E.; Browver, A. M.; Fitch, J. C.; Meyer, T. E.; van Grondelle, R.; Hellingwerf, K. J. *Biophys. J.* **1994**, *67*, 1691.
(8) Imamoto, Y.; Kataoka, M.; Tokunaga, F. *Biochemistry* **1996**, *35*, 14047.
(9) Ujj, L.; Devanathan, S.; Meyer, T. E.; Cusanovich, M. A.; Tollin, G.; Atkinson, G. H. *Biophys. J.* **1998**, *75*, 406.
(10) Takeshita, K.; Imamoto, Y.; Kataoka, M.; Tokunaga, F.; Terajima, M. *Biochemistry* **2002**, *41*, 3037.
(11) Chosrowjan, H.; Mataga, N.; Nakashima, N.; Imamoto, Y.; Tokunaga, F. *Chem. Phys. Lett.* **1997**, *270*, 267.
(12) Baltuska, A.; van Stokkum, I. H. M.; Kroon, A.; Monshouwer, R.; Hellingwerf, K. J.; van Grondelle, R. *Chem. Phys. Lett.* **1997**, *270*, 263.
(13) Changenet, P.; Zhang, H.; van der Meer, M. J.; Hellingwerf, K. J.; Glasbeek, M. *Chem. Phys. Lett.* **1998**, *282*, 276.
(14) Chosrowjan, H.; Mataga, N.; Shibata, Y.; Imamoto, Y.; Tokunaga, F. *J. Phys. Chem. B* **1998**, *102*, 7695.
(15) Mataga, N.; Chosrowjan, H.; Shibata, Y.; Imamoto, Y.; Tokunaga, F. *J. Phys. Chem. B* **2000**, *104*, 5191.
(16) Imamoto, Y.; Kataoka, M.; Tokunaga, F.; Asahi, T.; Masuhara, H. *Biochemistry* **2001**, *40*, 6047.
(17) Devanathan, S.; Pacheco, A.; Ujj, L.; Cusanovich, M.; Tollin, G.; Lin, S.;Woodbury, N. *Biophys. J.* **1999**, *77*, 1017.
(18) Mataga, N.; Chosrowjan, H.; Shibata, Y.; Imamoto, Y.; Kataoka, M.; Tokunaga, F. *Chem. Phys. Lett.* **2002**, *352*, 220.
(19) Chosrowjan, H.; Mataga, N.; Taniguchi, S.; Shibata, Y.; Hamada, N.; Tokunaga, F. Imamoto, Y.; Kataoka, M. *J. Photosci.* **2002**, *9*, 122.
(20) Mataga, N.; Chosrowjan, H.; Taniguchi, S.; Hamada, N.; Tokunaga, F.; Imamoto, Y.; Kataoka, M. *Phys. Chem. Chem. Phys.* **2003**, *5*, 2454.
(21) Gensch, T.; Gradinaru, C. C.; van Stokkum, I. H. M.; Hendricks, J.; Hellingwerf, K. J.; van Grondelle, R. *Chem. Phys. Lett.* **2002**, *356*, 347.
(22) Nakamura, R.; Kanematsu, Y.; Kumauchi, M.; Hamada, N.; Tokunaga, F. *J. Lumin.* **2003**, *102*−*103C*, 21.
(23) Yoshizawa, T.; Wald, G. *Nature* **1963**, *197*, 1279.
(24) Birge, R. R. *Annu. Rev. Phys. Chem.* **1990**, *41*, 683.
(25) Du, M.; Flemming, G. R. *Biophys. Chem.* **1993**, *48*, 101.
(26) Kochendoerfer, G. G.; Mathies, R. A. *Isr. J. Chem.* **1995**, *35*, 211.
(27) Chosrowjan, H.; Mataga, N.; Shibata, Y.; Tachibanaki, S.; Kandori, H.; Shichida, Y.; Okada, T.; Kouyama, T. *J. Am. Chem. Soc.* **1998**, *120*, 9706.
(28) Kandori, H.; Furutani, Y.; Nishimura, S.; Shichida, Y.; Chosrowjan, H.; Shibata, Y.; Mataga, N. *Chem. Phys. Lett.* **2001**, *334*, 271.
(29) Changenet-Barret, P.; Plaza, P.; Martin, M. M. *Chem. Phys. Lett.* **2001**, *336*, 439.
(30) Changenet-Barret, P.; Espagne, A.; Katsonis, N.; Charier, S.; Baudin, J.-B.; Jullien, L.; Plaza, P.; Martin, M. M. *Chem. Phys. Lett.* **2002**, *365*, 285.
(31) Genick, U. K.; Soltis, S. M.; Kuhn, P.; Canestrelli, I. L.; Getzoff, E. D. *Nature* **1998**, *392*, 206.
(32) Perman, B.; Srajer, V.; Ren, Z.; Teng, T.-Y.; Praderwand, C.; Ursby, T.; Bourgeois, D.; Schotte, F.; Wulff, M.; Kort, R.; Hellingwerf, K., J.; Moffat, K. *Science* **1998**, *279*, 1946.
(33) Imamoto, Y.; Mihara, K.; Hisatomi, O.; Kataoka, M.; Tokunaga, F.; Bojkova, N.; Yoshihara, K. *J. Biol. Chem.* **1997**, *272*, 12905.
(34) Unno, M.; Kumauchi, M.; Sasaki, J.; Tokunaga, F.; Yamauchi, S. *Biochemistry* **2002**, *41*, 5668.
(35) Yamada, A.; Yamamoto, S.; Yamato, T.; Kakitani, T. *THEOCHEM* **2001**, *536*, 195.
(36) (a) Hellingwerf, K. J.; Hendriks, J.; Gensch, T. *J. Phys. Chem. A* **2003**, *107*, 1082. (b) Cusanovich, M.; Meyer, T. E. *Biochemistry* **2003**, *42*, 4759.
(37) (a) Saltiel, J.; Megarity, E. D. *J. Am. Chem. Soc.* **1972**, *94*, 2742. (b) Hochstrasser, R. M. *Pure Appl. Chem.* **1980**, *52*, 2683. (c) Fleming, G. R. *Chemical Applications of Ultrafast Spectroscopy*; Oxford University Press: New York, 1986; p 179. (d) Note: This, however, may not be true when multiple excited states are involved.
(38) Kobayashi, T.; Saito, T.; Ohtani, H. *Nature* **2001**, *414*, 531.

(39) Unno, M.; Kumauchi, M.; Sasaki, J.; Tokunaga, F.; Yamauchi, S. *J. Phys. Chem. B* **2003**, *107*, 2837.

(40) Unno, M.; Kumauchi, M.; Sasaki, J.; Tokunaga, F.; Yamauchi, S. *J. Am. Chem. Soc.* **2000**, *122*, 4233.

(41) Kim, M.; Mathies, R. A.; Hoff, W. D.; Hellingwerf, K. J. *Biochemistry* **1995**, *33*, 12669.

(42) Brudler, R.; Meyer, T. E.; Genick, U. K.; Devanathan, S.; Woo, T. T.; Miller, D. P.; Gerwert, K.; Cusanovich, M. A.; Tollin, G.; Getzoff, E. D. *Biochemistry* **2000**, *39*, 13478.

(43) Zhou, Y.; Ujj, L.; Meyer, T. E.; Cusanovich, M. A.; Atkinson, G. H. *J. Phys. Chem. A* **2001**, *105*, 5719.

(44) William, S. W.; William, D. E., Jr. *J. Am. Chem. Soc.* **1961**, *83*, 1733.

(45) The subscripts "dark" and "L" (light) stand for ground and first long-lived (~200 μs) intermediate states of the PYP photocycle (referred in the literature also as pR or I_1), respectively. PYP_L builds up within several nanoseconds from the excited state (S_1) of the protein and should not be mistaken with it. Note also that the chromophore in PYP_{dark} is in the trans conformation, while in PYP_L, it is in the cis configuration.

(46) Koch, W.; Holthausen, M. C. *A Chemist's Guide to Density Functional Theory*; Wiley-VCH: Weinheim, 2000.

(47) Frisch, M. J.; Trucks, G. W.; Schlegel, H. B.; Scuseria, G. E.; Robb, M. A.; Cheeseman, J. R.; Zakrzewski, V. G.; Montgomery, J. A., Jr.; Stratmann, R. E.; Burant, J. C.; Dapprich, S.; Millam, J. M.; Daniels, A. D.; Kudin, K. N.; Strain, M. C.; Farkas, O.; Tomasi, J.; Barone, V.; Cossi, M.; Cammi, R.; Mennucci, B.; Pomelli, C.; Adamo, C.; Clifford, S.; Ochterski, J.; Petersson, G. A.; Ayala, P. Y.; Cui, Q.; Morokuma, K.; Malick, D. K.; Rabuck, A. D.; Raghavachari, K.; Foresman, J. B.; Cioslowski, J.; Ortiz, J. V.; Stefanov, B. B.; Liu, G.; Liashenko, A.; Piskorz, P.; Komaromi, I.; Gomperts, R.; Martin, R. L.; Fox, D. J.; Keith, T.; Al-Laham, M. A.; Peng, C. Y.; Nanayakkara, A.; Gonzalez, C.; Challacombe, M.; Gill, P. M. W.; Johnson, B. G.; Chen, W.; Wong, M. W.; Andres, J. L.; Head-Gordon, M.; Replogle, E. S.; Pople, J. A. *Gaussian 98*; Gaussian, Inc.: Pittsburgh, PA, 1998.

(48) Rubtsov, I. V.; Yoshihara, K. *J. Phys. Chem. A* **1999**, *103*, 10202.

(49) We note that it would be deceptive to Fourier transform numerically extracted oscillatory components alone because important details such as peak intensities in the transformed spectra depend sensitively on the method used to subtract off the underlying *nonexponential* excited-state population decay. Hence, we present in Figures 2 and 5 the DFTS of whole fluorescence transients.

(50) Mataga, N.; Chosrowjan, H.; Taniguchi, S.; Shibata, Y.; Yoshida, N.; Osuka, A.;Kikuzawa, T.; Okada, T. *J. Phys. Chem. A* **2002**, *106*, 12191.

(51) Mataga, N.; Chosrowjan, H.; Taniguchi, S.; Tanaka, F.; Kido, N.; Kitamura, M. *J. Phys. Chem. B* **2002**, *106*, 8917.

(52) van Aalten, D. M. F.; Crielaard, W.; Hellingwerf, K. J.; Joshua-Tor, L. *Acta Crystallogr. D* **2002**, *58*, 585.

(53) Cordfunke, R.; Kort, R.; Pierik, A.; Gobets, B.; Koomen, G. J.; Verhoeven, J. W.; Hellingwerf, K. J. *Proc. Natl. Acad. Sci.* **1998**, *95*, 7396.

(54) Jarzeba, W.; Walker, G. C.; Johnson, A. E.; Barbara, P. F. *Chem. Phys.* **1991**, *152*, 57.

(55) Our unpublished DFT calculations and RR experiments suggest that the NH_2 group of Q46 forms a H bond with the phenolic O^- of the chromophore, although the H-bond energy is smaller in E46Q mutant compared with that of native PYP.

(56) Mizutani, Y.; Kitagawa, T. *Science* **1997**, *278*, 443.

(57) The chromophore of PYP has the low symmetry C_s. Thus, there are only two A′ and A″ configurations, and the symmetry notations are not so useful in this case. Briefly, in common nomenclature, the notations γ and ν correspond to out-of-plane and in-plane vibrations, respectively, and the subscript numbers (1, 2, 3, ...) are numberings from higher to lower frequencies. However, because the number of atoms (also the number of normal modes) is different for the native and analogue chromophores, one should be careful when comparing modes with similar notations such as γ_{16} or ν_{43}. Thus, in our special case, the same notation was used for the similar mode regardless of its order, i.e., we used the notation of the HCMT[39] for the similar modes for both native chromophore model (HCET) as well as locked chromophore analogue model (HCCET) and the later modes are marked with a dash.

(58) Kroon, A. R.; Hoff, W. D.; Fennema, H.; Koomen, G. J.; Verhoeven, J. W.;Crielaard, W.; Hellingwerf, K. J. *J. Biol. Chem.* **1996**, *271*, 31949.

(59) We note that a principal difference between low-frequency in-plane and out-of-plane modes might not be very clear in the real PYP system; i.e., in the low-frequency region, almost all modes might contain both in-plane and out-of-plane characteristics.